Available online at www.sciencedirect.com
ScienceDirect
Applied Ocean Research 28 (2006) 407–419
Applied Ocean Research
www.elsevier.com/locate/apor

Fatigue damage in randomly vibrating jack-up platforms under non-Gaussian loads

Sayan Gupta[a,*,1], Naser Shabakhty[b,2], Pieter van Gelder[a,3]

[a] Department of Civil Engineering, Section of Hydraulic Engineering, Technical University of Delft, Stevinweg 1, PO BOX 5048, 2600 GA, Delft, The Netherlands
[b] Department of Civil Engineering, University of Sistan and Baluchestan, Zahedan, Iran

Received 7 July 2006; received in revised form 8 October 2006; accepted 2 February 2007
Available online 16 April 2007

Abstract

The problem of fatigue damage estimation of ageing jack-up platforms is considered, using theories of random processes. The sea-wave excitations are modelled as stationary, Gaussian random processes, with specified power spectral density function. The loads acting on the structure due to the sea waves is calculated using Morison's equation and are therefore non-Gaussian whose probabilistic properties are not available in explicit form. Assuming linear structure behaviour, the probabilistic properties of the structure response are determined using theories of random vibrations. The simple peak counting method is adopted for estimating the mean fatigue damage. This requires knowledge of the joint probability density function of the structure response and its first and second time derivatives, at the same time instant. A methodology has been presented for developing analytical expressions for this joint pdf. This requires evaluation of multidimensional integrals. A recently developed computational algorithm is presented to deal with integrals for which derivation of closed form analytical expressions may not be feasible. The methodology proposed in this paper provides an alternative and computationally cheaper technique for estimating the fatigue damage in comparison to the Monte Carlo simulation procedure. Numerical results have been presented for illustration of the proposed methodology.

Keywords: Random fatigue; Offshore structures; Random vibrations; Peak distributions; non-Gaussian processes

1. Introduction

Jack-up platforms are used for exploration and extraction of hydrocarbons from the ocean beds. These are large movable structures, which have been designed to operate at various locations with differing sea-bed conditions, great water depths and under various sea conditions. Over the last few decades, the offshore industry has ventured into deeper waters and more severe sea conditions. This has subjected the jack-up platforms to severe environments. Consequently, this has led to increased scrutiny about the safety of these structures. Usually built at massive costs, there is therefore considerable interest in estimating the lifetime of jack-up platforms and devising efficient maintenance schedules which increase their life span without compromising on their usefulness or safety. This necessitates the development of efficient tools for quantifying the ageing process of these structures.

Structural ageing is a phenomenon characterized by structural degradation due to various phenomena, arising from effects such as corrosion from the sea water, differences in temperature, creep effects, fatigue damage due to the dynamic effects of sea waves and wind and mechanical damage due to accidental impacts with ships and other marine vessels. In this study, we focus our attention on estimating the fatigue damage for jack-up platforms due to the impact of the sea-waves.

Estimating the fatigue damage for offshore structures is a complicated problem, requiring accurate dynamic analysis of these structures, under sea-wave loadings. The analysis usually relies on a number of simplifying assumptions on the forces caused by the sea waves, the structural behaviour and the models for the structures. Thus, often, simple linear wave

* Corresponding author. Tel.: +31 15 27 88256; fax: +31 15 27 85 124.
E-mail addresses: gupta.sayan@gmail.com, S.Gupta@tudelft.nl (S. Gupta), shabakhty@yahoo.com (N. Shabakhty), P.H.A.J.M.vanGelder@tudelft.nl (P. van Gelder).
1 Post-doctoral Researcher.
2 Assistant Professor.
3 Assistant Professor.

0141-1187/$ - see front matter © 2007 Elsevier Ltd. All rights reserved.
doi:10.1016/j.apor.2007.02.001

theories are used where the sea elevations are assumed to be stationary, Gaussian processes and the structure behaviour is assumed to be linear. However, the increased loads on the offshore structures due to the venturing out of the industry to deeper waters has necessitated studies which address the complicating features arising from nonlinear waves and structural nonlinear behaviour. Thus, studies on nonlinear sea conditions [1–5] and consequent structural behavior [6–11] have been discussed in the literature. Questions arising from the nonlinear structural behaviour have been addressed using methods based on equivalent linearization and frequency domain expansions using transfer functions [12–17].

As in many areas of random vibrations, estimates of the expected fatigue damage may be obtained via the Monte Carlo method [18]. The Monte Carlo method basically involves digital generation of an ensemble of random loads, repeated deterministic analysis of a structure subjected to each sample loading and statistical processing of the results obtained from each deterministic analysis. It is well established that the Monte Carlo method offers the best accuracy subject to the limitations of the sample size considered in the analysis. However, high computational costs and large data storage requirements often prove to be major limitations in implementation of this technique. This is particularly true in random fatigue analysis, which usually involves repeated analysis of long time histories. On the other hand, analytical methods, though often built on certain assumptions, provide elegant and easy to compute solutions, which have acceptable levels of accuracy.

In this paper, we develop a frequency domain-based technique for calculating the expected fatigue damage in randomly vibrating jack-up platforms. The sea-wave elevations are assumed to be modelled as stationary Gaussian random processes. The forces acting on the structure are calculated using the well-known Morison's equations and are non-Gaussian in nature. Consequently, the stresses developed in the structure are also non-Gaussian, whose probability density functions (pdf) are not available in explicit forms. The fatigue damage is computed using the peak counting method [19,20]. This, in turn, requires the knowledge of the distribution of the peaks for the stresses developed in the structure [21–23]. The focus of this paper is on developing analytical approximations for the peak distributions for the random stress components. This, in turn, implies the need for developing approximations for the joint pdf of the non-Gaussian process (stress), and its first and second time derivatives, at any time instant. In this paper, we propose an analytical method to develop approximations for the joint pdf of the non-Gaussian process, and its first and second time derivatives. Techniques for approximating these expressions have been developed recently [24]. The underlying principles of this method had been originally proposed, in the context of extreme value distributions for a limited class of problems [25] and recently, had been extended by the present authors to include a wider class of problems [24,26]. The approximations for the joint pdf, in turn, lead to analytical expressions for the pdf of the peaks for the non-Gaussian stresses. These expressions are subsequently used in estimating the expected fatigue damage, when the peak counting method is employed for estimating the mean fatigue damage due to random dynamic loads.

2. Problem statement

A jack-up platform subjected to Gaussian sea excitations is considered. We assume that the structure behaviour is linear. If the structure is discretized using finite elements (FE), the discretized form of the governing equations of motion can be represented as

$$\mathbf{M}\ddot{\mathbf{X}}(t) + \mathbf{C}\dot{\mathbf{X}}(t) + \mathbf{K}\mathbf{X}(t) = \mathbf{F}(t), \tag{1}$$

where, $\mathbf{M}$, $\mathbf{C}$ and $\mathbf{K}$ are the structure mass, damping and stiffness matrices of dimensions $n \times n$, $\ddot{\mathbf{X}}(t)$, $\dot{\mathbf{X}}(t)$ and $\mathbf{X}(t)$ are n-dimensional vectors for the accelerations, velocities and displacements of the structure at its nodes respectively, t is time and $\mathbf{F}(t)$ is the n-dimensional vector for the nodal forces. Since a jack-up platform typically has multiple legs which are subjected to wave loading, the problem being considered is essentially a multiple excitation problem. It must be noted that the variation of the velocity of the water particle along the depth of each of the supports is assumed to be deterministic. Thus, if the force imparted on a support is assumed to be $f(t)$ at a particular reference point, the variation of the force along the vertical axis of the support is given by $\mathbf{\Lambda} f(t)$. Here, $f(t)$ is assumed to be random process, and $\mathbf{\Lambda}$ is a deterministic vector which models the wave force variation with the depth. More details on $\mathbf{\Lambda}$ is given in Section 7.

The force $f(t)$ imparted on the reference point can be calculated using the well-known Morison's equations [27]. It can be shown that

$$f(t) = f_I(t) + f_D(t), \tag{2}$$

where, $f_I(t)$ is the inertial force per unit length, due to water particle acceleration and $f_D(t)$ is the force arising due to hydrodynamic drag, per unit length. Mathematically, these are represented as

$$f_I(t) = C_M \rho \frac{\pi D^2}{4} \dot{u}(t), \tag{3}$$

$$f_D(t) = \frac{1}{2} C_D \rho D |u(t)| u(t), \tag{4}$$

where, $u(t)$ and $\dot{u}(t)$ are respectively the water particle velocity and accelerations, modelled as random processes in time, D is the diameter of the cylindrical platform supports, ρ is the density of the water and C_M and C_D are respectively, the inertial and drag coefficients. The effect of structural damping is approximately accounted for by introducing hydrodynamic damping, such that, the total damping contribution from the structural damping and the hydrodynamic damping is about 5%. In calculating $f_D(t)$, we assume that the structure is stiff and we ignore the effect of the relative velocity due to the movement of the structural member. The effect of load intermittency in the splash zone is not considered either. The effect of added mass has been however incorporated.

The fatigue damage at a particular location of the structure occurs due to stress reversals. We assume that the stress resultant $Y(t)$ at a particular location (FE node) of the structure be expressible as a linear function of the corresponding displacement $X(t)$ at that node. We further assume that the fatigue damage due to $Y(t)$ can be expressed through the well known Palmgren-Miner's hypothesis [20]. Here, the accumulated linear fatigue damage caused by $Y(t)$, $t \in [0, T]$, is denoted by D_T, and is given by $D_T = \sum \alpha S_j^\beta$, where, α, ($\alpha > 1$) and β are material properties, determined from experiments, S denotes the stress levels for the counted cycles and the counter j indicates the number of equivalent stress cycles corresponding to an appropriate cycle counting scheme, within the time duration $[0, T]$. In this study, we assume the peak counting method in computing the fatigue damage and thus, the maximum value j takes is equal to the total number of peaks for $Y(t)$ in $[0, T]$. Since $Y(t)$ is a random process, D_T is a random variable. If $Y(t)$ is a stationary process, $D_T/T = d$ is the fatigue damage per unit time, and is also a random variable. It can be shown that when the mean stress effect is neglected, the expected fatigue damage per unit time, $\mathsf{E}[d]$, is given by the relation [28]

$$\mathsf{E}[d] = \nu_a \alpha \int_0^\infty s^\beta p_a(s; t)\mathrm{d}s. \tag{5}$$

Here, $p_a(\cdot)$ is the pdf of the random amplitude levels, a, and ν_a is the mean rate of occurrence for the cycles. Since for a complete cycle, each cycle is associated with a peak, $\nu_a = \nu_p$, where ν_p is the mean occurrence rate of peaks [29]. In the peak counting method it is assumed that the damage is related to the peak distribution, $p_p(\cdot)$, because its positive part agrees with the amplitude distribution. Thus, one can rewrite Eq. (5) as

$$\mathsf{E}[d] = \tilde{\nu}_p \alpha \int_0^\infty s^\beta p_p(s; t)\mathrm{d}s. \tag{6}$$

It must be noted here that $\tilde{\nu}_p$ denotes the mean occurrence rate of positive peaks only and is different from ν_p. This correction is necessary since in Eq. (6), the peaks below zero are neglected, and hence, the expected number of cycles ν_a is lower than the expected number of peaks. Thus, to estimate $\mathsf{E}[d]$, one needs first to compute $\tilde{\nu}_p$ and $p_p(\cdot)$.

The occurrence of a peak for $Y(t)$, at time t, above a threshold value y, can be mathematically represented as the event, such that

$$\begin{aligned} &Y(t) > y \\ &\dot{Y}(t) = 0, \\ &\ddot{Y}(t) < 0. \end{aligned} \tag{7}$$

Thus, one can see that the occurrence of a peak involves a zero-level down-crossing of the process derivative $\dot{Y}(t)$ at the same time instant. Thus, ν_p can be calculated by application of the well-known Rice's formula [30]

$$\begin{aligned} \nu_p &= -\int_{-\infty}^0 \ddot{y} p_{\dot{Y}\ddot{Y}}(0, \ddot{y}; t)\mathrm{d}\ddot{y} \\ &= -\int_{-\infty}^\infty \int_{-\infty}^0 \ddot{y} p_{Y\dot{Y}\ddot{Y}}(y, 0, \ddot{y}; t)\mathrm{d}\ddot{y}\mathrm{d}y. \end{aligned} \tag{8}$$

Here, $p_{Y\dot{Y}\ddot{Y}}(y, \dot{y}, \ddot{y}; t)$ is the joint pdf for $Y(t)$, $\dot{Y}(t)$ and $\ddot{Y}(t)$, at time t. However, if one discounts for the negative peaks, we get

$$\tilde{\nu}_p = -\int_0^\infty \int_{-\infty}^0 \ddot{y} p_{Y\dot{Y}\ddot{Y}}(y, 0, \ddot{y}; t)\mathrm{d}\ddot{y}\mathrm{d}y. \tag{9}$$

It is obvious from Eqs. (8) and (9) that $\tilde{\nu}_p \le \nu_p$.

The probability distribution function (PDF) for the peaks of $Y(t)$, above a threshold level y, is given by [21–23]

$$P[p \le y] = 1 - \frac{1}{\nu_p} \int_y^\infty \int_{-\infty}^0 \ddot{y} p_{Y\dot{Y}\ddot{Y}}(y, 0, \ddot{y}; t)\mathrm{d}\ddot{y}\mathrm{d}y, \tag{10}$$

where, p is the random variable denoting the peaks of $Y(t)$. The corresponding pdf for p is given by

$$p_p(y; t) = -\frac{1}{\nu_p} \int_{-\infty}^0 \ddot{y} p_{Y\dot{Y}\ddot{Y}}(y, 0, \ddot{y}; t)\mathrm{d}\ddot{y}. \tag{11}$$

Since $f(t)$ in Eq. (2) is non-Gaussian, the structure response $Y(t)$ is non-Gaussian, whose pdf is difficult to estimate. The knowledge of the joint pdf $p_{Y\dot{Y}\ddot{Y}}(\cdot)$ is not available either. The focus of this study is to first, obtain approximations for $p_{Y\dot{Y}\ddot{Y}}(\cdot)$ and subsequently, develop approximations for the expected fatigue damage rate, $\mathsf{E}[d]$.

3. Representing the second order response

We first consider the forces acting on one of the supports of the jack-up platform. We assume that the water particle velocity $u(t)$ at the reference level is a stationary Gaussian random process, with specified mean u_0 and a zero-mean Gaussian random component $\zeta(t)$, with specified one-sided power spectral density (PSD) $S_{\zeta\zeta}(\omega)$. We define the Gaussian process $\zeta(t)$, in the limit as N tends to infinity, to be of the form

$$\zeta_N(t) = \sum_{j=-N}^{N} \frac{\sigma_j}{2}(U_j - \mathrm{i}V_j)\mathrm{e}^{\mathrm{i}\omega_j t}, \tag{12}$$

where, U_j, V_j, $j > 0$ are independent standard normal random variables and $U_{-j} = U_j$, $V_{-j} = -V_j$, $\omega_{-j} = -\omega_j = j\omega_c/N$ and $\sigma_j^2 = S_{\zeta\zeta}(\omega_j)\Delta\omega$. Here, $j = 1, \ldots, N$, $\sigma_0 = 0$, $\Delta\omega = \omega_c/N$, ω is frequency defined in $0 \le \omega \le \omega_c$ and ω_c is the cut-off frequency, such that, $S_{\zeta\zeta}(\omega) = 0$, if $\omega > \omega_c$. For the sake of simplicity, we write $\zeta(t)$ instead of $\zeta_N(t)$. The corresponding expression for the water particle acceleration is given by

$$\dot{\zeta}(t) = \sum_{j=-N}^{N} \mathrm{i}\omega_j \frac{\sigma_j}{2}(U_j - \mathrm{i}V_j)\mathrm{e}^{\mathrm{i}\omega_j t}. \tag{13}$$

We substitute Eqs. (12) and (13) into Eqs. (2)–(4). Here, $u(t) = u_0 + \zeta(t)$. The forcing function $f(t)$ can be expressed as a summation of a linear component, $f_L(t)$ and a quadratic component, $f_Q(t)$. The expressions for these components, however, depend on the sign of $u(t)$. Note that the term associated with u_0^2 do not contribute to the dynamic effects (and hence do not affect fatigue damage when mean effects are ignored) and are neglected from the analysis.

Thus, we get

$$f_L^+(t) = \sum_{j=-N}^{N} (\mathrm{i}\omega_j A_I + 2u_0 A_D)\frac{\sigma_j}{2}(U_j - \mathrm{i}V_j)\mathrm{e}^{\mathrm{i}\omega_j t}, \quad \text{if } u(t) > 0,$$
$$f_L^-(t) = \sum_{j=-N}^{N} (\mathrm{i}\omega_j A_I - 2u_0 A_D)\frac{\sigma_j}{2}(U_j - \mathrm{i}V_j)\mathrm{e}^{\mathrm{i}\omega_j t}, \quad \text{if } u(t) < 0, \tag{14}$$

and

$$f_Q^+(t) = A_D \sum_{j=-N}^{N}\sum_{k=-N}^{N} \frac{\sigma_j\sigma_k}{4}(U_j - \mathrm{i}V_j)(U_k + \mathrm{i}V_k) \times \mathrm{e}^{\mathrm{i}(\omega_j-\omega_k)t}, \quad \text{if } u(t) > 0, \tag{15}$$
$$f_Q^-(t) = -A_D \sum_{j=-N}^{N}\sum_{k=-N}^{N} \frac{\sigma_j\sigma_k}{4}(U_j - \mathrm{i}V_j)(U_k + \mathrm{i}V_k) \times \mathrm{e}^{\mathrm{i}(\omega_j-\omega_k)t}, \quad \text{if } u(t) < 0.$$

Here, $A_I = C_M\rho\frac{\pi D^2}{4}$, $A_D = \frac{1}{2}C_D\rho D$ are constants and the superscripts $+$ and $-$ in Eqs. (14) and (15) indicate the sign of $u(t)$.

Since structure behavior is assumed to be linear, the structure response $Y(t)$ in the discretized form can be written as the summation of a linear term, $Y_L(t)$ and a quadratic term $Y_Q(t)$, which are expressed as

$$Y_L^+(t) = \sum_{j=-N}^{N} (\mathrm{i}\omega_j A_I + 2u_0 A_D)\hat{H}_1(\omega_j)\frac{\sigma_j}{2}(U_j - \mathrm{i}V_j)\mathrm{e}^{\mathrm{i}\omega_j t}, \quad \text{if } u(t) > 0,$$
$$Y_L^-(t) = \sum_{j=-N}^{N} (\mathrm{i}\omega_j A_I - 2u_0 A_D)\hat{H}_1(\omega_j)\frac{\sigma_j}{2}(U_j - \mathrm{i}V_j)\mathrm{e}^{\mathrm{i}\omega_j t}, \quad \text{if } u(t) < 0, \tag{16}$$

and

$$Y_Q^+(t) = A_D \sum_{j=-N}^{N}\sum_{k=-N}^{N} \hat{H}_2(\omega_j, -\omega_k)\frac{\sigma_j\sigma_k}{4} \times (U_j - \mathrm{i}V_j)(U_k + \mathrm{i}V_k)\mathrm{e}^{\mathrm{i}(\omega_j-\omega_k)t}, \quad \text{if } u(t) > 0,$$
$$Y_Q^-(t) = -A_D \sum_{j=-N}^{N}\sum_{k=-N}^{N} \hat{H}_2(\omega_j, -\omega_k)\frac{\sigma_j\sigma_k}{4} \times (U_j - \mathrm{i}V_j)(U_k + \mathrm{i}V_k)\mathrm{e}^{\mathrm{i}(\omega_j-\omega_k)t}, \quad \text{if } u(t) < 0. \tag{17}$$

As before the superscripts $+$ and $-$ in Eqs. (16) and (17) indicate the expressions corresponding the appropriate sign of $u(t)$. Here, $\hat{H}_1(\omega)$ is the linear transfer function for the structural response at the desired location, when a unit force acts at the point of application of $f_1(t)$. $\hat{H}_2(\omega_1, \omega_2)$ is the corresponding quadratic transfer function, given by $\hat{H}_2(\omega_1, \omega_2) = \hat{H}_1(\omega_1 + \omega_2)$.

Now, a particular support of the jack-up platform, is subjected to forces simultaneously at all the nodes submerged in water. Let the water particle velocity at depth z be $\zeta_z(t)$ and the corresponding force acting on the node at depth z be represented by $f_z(t)$. Let us also assume that in the frequency domain, one can write $\zeta_z(\omega) = \tilde{g}_z(\omega)\zeta(\omega)$, where $\zeta(\omega)$ is the Fourier transform of $\zeta(t)$ in Eq. (12). The reasoning behind writing $\zeta_z(\omega)$ in the above form will be made clear later in Section 7. Here, $\tilde{g}_z(\omega)$ behaves as a deterministic scaling function. The structure response corresponding to this force can be written in similar form as in Eqs. (16) and (17), but with the terms within the summation signs being multiplied with the following terms: $\tilde{g}_z(\omega_j)$ for Eq. (16), and $\tilde{g}_z(\omega_j)\tilde{g}_z(-\omega_k)$ for Eq. (17). Here, the transfer functions $\hat{H}_1(\omega)$ and $\hat{H}_2(\omega_1, \omega_2)$ correspond to the linear and quadratic transfer functions for the response, when a unit load acts on the point of application of $f_z(t)$. Since structure linear behavior is assumed, the total response due to all the forces acting on one of the supports is the summation of their individual responses and can be written as

$$Y_L^+(t) = \sum_{j=-N}^{N} (\mathrm{i}\omega_j A_I + 2u_0 A_D)H_1(\omega_j)\frac{\sigma_j}{2}(U_j - \mathrm{i}V_j)\mathrm{e}^{\mathrm{i}\omega_j t}, \quad \text{if } u(t) > 0,$$
$$Y_L^-(t) = \sum_{j=-N}^{N} (\mathrm{i}\omega_j A_I - 2u_0 A_D)H_1(\omega_j)\frac{\sigma_j}{2}(U_j - \mathrm{i}V_j)\mathrm{e}^{\mathrm{i}\omega_j t}, \quad \text{if } u(t) < 0, \tag{18}$$

and

$$Y_Q^+(t) = A_D \sum_{j=-N}^{N}\sum_{k=-N}^{N} H_2(\omega_j, -\omega_k)\frac{\sigma_j\sigma_k}{4} \times (U_j - \mathrm{i}V_j)(U_k + \mathrm{i}V_k)\mathrm{e}^{\mathrm{i}(\omega_j-\omega_k)t}, \quad \text{if } u(t) > 0,$$
$$Y_Q^-(t) = -A_D \sum_{j=-N}^{N}\sum_{k=-N}^{N} H_2(\omega_j, -\omega_k)\frac{\sigma_j\sigma_k}{4} \times (U_j - \mathrm{i}V_j)(U_k + \mathrm{i}V_k)\mathrm{e}^{\mathrm{i}(\omega_j-\omega_k)t}, \quad \text{if } u(t) < 0. \tag{19}$$

Here, $H_1(\omega_j) = H_{11}(\omega_j) + \tilde{g}_{z_1}(\omega_j)H_{1z_1}(\omega_j) + \cdots + \tilde{g}_{z_m}(\omega_j)H_{1z_m}(\omega_j)$, $H_2(\omega_j, -\omega_k) = H_{11}(\omega_j - \omega_k) + \tilde{g}_{z_1}(\omega_j)\tilde{g}_{z_1}(-\omega_k)H_{1z_1}(\omega_j - \omega_k) + \cdots + \tilde{g}_{z_m}(\omega_j)\tilde{g}_{z_m}(-\omega_k)H_{1z_m}(\omega_j - \omega_k)$, m is the total number of submerged nodes in one support of the jack-up platform and $H_{1j}(\omega)$ denotes the linear transfer function for the structure response (at the desired node) when a unit force is applied at the j-th submerged node.

Now, if the structure response of interest is at the i-th node, $H_{1z}(\omega)$ is obtained from the i-th entry of the vector given by

$$\{\mathbf{H}_{1z}(\omega)\}_i = [-\omega^2\mathbf{M} + \mathrm{i}\omega\mathbf{C} + \mathbf{K}]^{-1}\mathbf{F}_1(\omega), \tag{20}$$

where, $\mathbf{F}_1(\omega)$ is a zero vector with a unit load at the node corresponding to depth z. More discussions on this is available in Section 7.

We next define

$$\mathbf{\Theta}(t) = [(U_1 - \mathrm{i}V_1)\mathrm{e}^{\mathrm{i}\omega_1 t} \ldots (U_N - \mathrm{i}V_N)\mathrm{e}^{\mathrm{i}\omega_N t}]', \tag{21}$$

where, the superscript ($'$) denotes the matrix transpose. We also introduce a column vector

$$\mathbf{Z}(t) = \begin{bmatrix} \Re(\boldsymbol{\Theta}(t)) \\ \Im(\boldsymbol{\Theta}(t)) \end{bmatrix}'. \tag{22}$$

Here, $\Re(\cdot)$ and $\Im(\cdot)$ denote the real and imaginary parts of the arguments. Introducing the notations

$$\mathbf{q}^+ = \Big[(\mathrm{i}\omega_1 A_I + 2A_D u_0)\frac{\sigma_1}{2}H_1(\omega_1), \ldots, (\mathrm{i}\omega_N A_I + 2A_D u_0) \times \frac{\sigma_N}{2}H_1(\omega_N)\Big], \tag{23}$$

$$\mathbf{q}^- = \Big[(\mathrm{i}\omega_1 A_I - 2A_D u_0)\frac{\sigma_1}{2}H_1(\omega_1), \ldots, (\mathrm{i}\omega_N A_I - 2A_D u_0) \times \frac{\sigma_N}{2}H_1(\omega_N)\Big], \tag{24}$$

the linear part of the response can be written as

$$Y_L^+ = \mathbf{A}_\mathbf{L}^+\mathbf{Z}(t), \quad \text{if } u(t) > 0,$$
$$Y_L^- = \mathbf{A}_\mathbf{L}^-\mathbf{Z}(t), \quad \text{if } u(t) < 0, \tag{25}$$

where, $\mathbf{A}_\mathbf{L}^+ = [\Re(\mathbf{q}^+)\Im(\mathbf{q}^+)]$ and $\mathbf{A}_\mathbf{L}^- = [\Re(\mathbf{q}^-)\Im(\mathbf{q}^-)]$ are vectors of length $2N \times 1$. To write the quadratic response using the $\mathbf{Z}(t)$ process. we define the following matrices:

$$\begin{aligned}
&\mathbf{Q}^+ = [Q_{mn}^+]; \qquad Q_{mn}^+ = A_D H_2(\omega_m, -\omega_n)\sigma_m\sigma_n,\\
&\mathbf{Q}^- = [Q_{mn}^-]; \qquad Q_{mn}^- = -A_D H_2(\omega_m, -\omega_n)\sigma_m\sigma_n,\\
&\mathbf{R}^+ = [R_{mn}^+]; \qquad R_{mn}^+ = A_D H_2(\omega_m, \omega_n)\sigma_m\sigma_n,\\
&\mathbf{R}^- = [R_{mn}^-]; \qquad R_{mn}^- = -A_D H_2(\omega_m, \omega_n)\sigma_m\sigma_n,\\
&\mathbf{W} = [W_{mn}], \qquad W_{mn} = -\omega_m \quad \text{if } m = n, \text{ and}\\
&W_{mn} = 0 \quad \text{if } m \neq n,
\end{aligned} \tag{26}$$

where, $m, n = 1, \ldots, N$. Introducing the following matrices of size: $2N \times 2N$,

$$\mathbf{A}_\mathbf{Q}^+ = \begin{bmatrix} \Re(\mathbf{Q}^+) + \Re(\mathbf{R}^+) & \Im(\mathbf{Q}^+) - \Im(\mathbf{R}^+) \\ \Im(\mathbf{Q}^+)' - \Im(\mathbf{R}^+)' & \Re(\mathbf{Q}^+) - \Re(\mathbf{R}^+) \end{bmatrix},$$
$$\mathbf{A}_\mathbf{Q}^- = \begin{bmatrix} \Re(\mathbf{Q}^-) + \Re(\mathbf{R}^-) & \Im(\mathbf{Q}^-) - \Im(\mathbf{R}^-) \\ \Im(\mathbf{Q}^-)' - \Im(\mathbf{R}^-)' & \Re(\mathbf{Q}^-) - \Re(\mathbf{R}^-) \end{bmatrix} \tag{27}$$

the quadratic responses can be written as

$$Y_Q^+(t) = \frac{1}{2}\mathbf{Z}(t)'\mathbf{A}_\mathbf{Q}^+\mathbf{Z}(t), \quad \text{if } u(t) > 0$$
$$Y_Q^-(t) = \frac{1}{2}\mathbf{Z}(t)'\mathbf{A}_\mathbf{Q}^-\mathbf{Z}(t), \quad \text{if } u(t) < 0. \tag{28}$$

Consequently, the response $Y(t)$ can now be expressed as a nonlinear function of $2N$ independent, zero-mean, unit variance processes $\{Z_i(t)\}_{i=1}^{2N}$, as follows:

$$Y(t) = \left\{ \begin{aligned} g^+(\mathbf{Z}(t)) = \mathbf{A}_\mathbf{L}^+\mathbf{Z}(t) + \frac{1}{2}\mathbf{Z}(t)'\mathbf{A}_\mathbf{Q}^+\mathbf{Z}(t), \ \text{if } u(t) > 0 \\ g^-(\mathbf{Z}(t)) = \mathbf{A}_\mathbf{L}^-\mathbf{Z}(t) + \frac{1}{2}\mathbf{Z}(t)'\mathbf{A}_\mathbf{Q}^-\mathbf{Z}(t), \ \text{if } u(t) < 0. \end{aligned} \right\} \tag{29}$$

Eq. (29) can be written as a single equation in the form

$$\begin{aligned} Y(t) &= g^+(\mathbf{Z}(t))\mathrm{U}[u(t)] + g^-(\mathbf{Z}(t))\mathrm{U}[-u(t)] \\ &= g(\mathbf{Z}(t)), \end{aligned} \tag{30}$$

where, the operator $\mathrm{U}[\cdot]$ is the Heaviside function and takes a value of unity if the argument is positive and zero otherwise. The covariance matrix between $\mathbf{Z}(t)$, $\dot{\mathbf{Z}}(t)$ and $\ddot{\mathbf{Z}}(t)$ is given by

$$\mathrm{Cov}[\mathbf{Z}(0), \dot{\mathbf{Z}}(0), \ddot{\mathbf{Z}}(0)] = \begin{bmatrix} \mathbf{I} & \mathbf{0} & \mathbf{0} & -\mathbf{W} & -\mathbf{W}^2 & \mathbf{0} \\ \mathbf{0} & \mathbf{I} & \mathbf{W} & \mathbf{0} & \mathbf{0} & -\mathbf{W}^2 \\ \mathbf{0} & \mathbf{W} & \mathbf{W}^2 & \mathbf{0} & \mathbf{0} & -\mathbf{W}^3 \\ -\mathbf{W} & \mathbf{0} & \mathbf{0} & \mathbf{W}^2 & \mathbf{W}^3 & \mathbf{0} \\ -\mathbf{W}^2 & \mathbf{0} & \mathbf{0} & \mathbf{W}^3 & \mathbf{W}^4 & \mathbf{0} \\ \mathbf{0} & -\mathbf{W}^2 & -\mathbf{W}^3 & \mathbf{0} & \mathbf{0} & \mathbf{W}^4 \end{bmatrix} \tag{31}$$

where, the first two rows and columns correspond to $\mathbf{Z}(t)$, the next two rows and columns correspond to $\dot{\mathbf{Z}}(t)$ and the last two rows and columns are for $\ddot{\mathbf{Z}}(t)$, $\mathbf{I}$ is an identity matrix of size $N \times N$ and $\mathbf{0}$ is a $N \times N$ matrix with all elements equal to zero. An approximation for the joint pdf $p_{Y\dot{Y}\ddot{Y}}(\cdot)$ can now be obtained using a recently developed technique, once $Y(t)$ is expressed as in Eq. (30). This will be discussed later in the paper.

4. Response due to multiple forces acting on the supports

Eq. (30) represents the response of the structure, at the desired location, due to the forces acting on one of the supports of the jack-up platform, and may be designated as $Y_i(t)$, where the suffix i denotes the i-th support. Since structure behaviour is linear, the superposition rule may be employed to compute the structure response due to the forces acting on all the supports. Mathematically, this may be represented as

$$Y(t) = \sum_{i=1}^{n_s} Y_i(t) = \sum_{i=1}^{n_s} g_i(\mathbf{Z}_i(t)), \tag{32}$$

where, n_s is the total number of supports. Here, it must be noted that not all the $\{Z_i(t)\}_{i=1}^{2Nns}$ are mutually independent processes. This is because the velocity components $\{\zeta_i(t)\}_{i=1}^{ns}$ acting on the various supports ($i = 1, \ldots, n_s$) are not independent.

Let us assume that $\mathbf{C}_{\zeta\zeta}(\tau)$ represents the $n_s \times n_s$ covariance matrix for the velocity components $\zeta(t) = \{\zeta_i(t)\}_{i=1}^{n_s}$, none of which are perfectly correlated to any other component. $\mathbf{C}_{\zeta\zeta}(\tau)$ is real, symmetrical and positive definite and can be written as

$$\mathbf{C}_{\zeta\zeta}(\tau) = \mathsf{E}[\zeta(t)\zeta(t+\tau)] = \boldsymbol{\Psi}\boldsymbol{\Upsilon}(\boldsymbol{\tau})\boldsymbol{\Psi}', \tag{33}$$

where, $\boldsymbol{\Upsilon}$ is a $n_s \times n_s$ diagonal matrix containing the eigenvalues of $\mathbf{C}_{\zeta\zeta}(\tau)$ (which are all real) and $\boldsymbol{\Psi}$ is a $n_s \times n_s$ matrix containing the ortho-normal vectors of $\mathbf{C}_{\zeta\zeta}(\tau)$. This implies that $\zeta(t) = \Psi^{-1}\Upsilon^{0.5}(t)$ where, $\Upsilon^{0.5}(t)$ can be visualized as random processes which are independent of each other.

Thus, given a vector of correlated random processes $\{\zeta_i(t)\}_{i=1}^{n_s}$, the above transformation can be applied to determine processes which are mutually independent. Subsequently, the transformations in Section 3 can be applied to represent $Y(t) = g(\{\mathbf{Z}_i(t)\}_{i=1}^{2Nn_s})$, where, $\mathbf{Z}(t)$ is a vector of mutually independent random processes of length $k = 2Nn_s \times 1$. The corresponding covariance matrices for $\mathbf{Z}(t)$, $\dot{\mathbf{Z}}(t)$ and $\ddot{\mathbf{Z}}(t)$ are more complicated than in Eq. (31) and is given by

$$\mathrm{Cov}[\mathbf{Z}(0), \dot{\mathbf{Z}}(0), \ddot{\mathbf{Z}}(0)] = \mathbf{\Psi}' \begin{bmatrix} \mathbf{I} & \mathbf{0} & \mathbf{0} & -\mathbf{W} & -\mathbf{W}^2 & \mathbf{0} \\ \mathbf{0} & \mathbf{I} & \mathbf{W} & \mathbf{0} & \mathbf{0} & -\mathbf{W}^2 \\ \mathbf{0} & \mathbf{W} & \mathbf{W}^2 & \mathbf{0} & \mathbf{0} & -\mathbf{W}^3 \\ -\mathbf{W} & \mathbf{0} & \mathbf{0} & \mathbf{W}^2 & \mathbf{W}^3 & \mathbf{0} \\ -\mathbf{W}^2 & \mathbf{0} & \mathbf{0} & \mathbf{W}^3 & \mathbf{W}^4 & \mathbf{0} \\ \mathbf{0} & -\mathbf{W}^2 & -\mathbf{W}^3 & \mathbf{0} & \mathbf{0} & \mathbf{W}^4 \end{bmatrix} \mathbf{\Psi}, \quad (34)$$

and are usually fully populated.

It is to be remarked here that the the assumption that the variation of the water particle velocity along the vertical axis of the supports being deterministic is not restrictive. Indeed, the water particle velocities acting on the nodes along the vertical axis of a support may be considered to be correlated random processes. The procedure described in this section can then be employed to represent the response $Y(t)$ as a nonlinear function of a vector of independent random processes $\mathbf{Z}(t)$.

5. Approximating the joint pdf $p_{Y\dot{Y}\ddot{Y}}(\cdot)$

The structure response and the first and second time derivatives, in terms of $\mathbf{Z}$, are given by

$$Y(t) = g[Z_1, \ldots, Z_k], \quad (35)$$

$$\dot{Y}(t) = \sum_{j=1}^{k} g'_j \dot{Z}_j(t), \quad (36)$$

$$\ddot{Y}(t) = \sum_{i=1}^{k}\sum_{j=1}^{k} g''_{ij} \dot{Z}_i(t)\dot{Z}_j(t) + \sum_{j=1}^{k} g'_j \ddot{Z}_j(t). \quad (37)$$

Here, g'_j and g''_{ij} are, respectively, the first and second derivatives of $g[\cdot]$ with respect to the components of $\mathbf{Z}$.

To proceed, we introduce a set of transformations that had first been introduced in [25], with relation to the study of extremes of random processes. Using similar principles, we now rewrite

$$p_{Y\dot{Y}\ddot{Y}}(y, 0, \ddot{y}; t) = \int_{-\infty}^{\infty} \cdots \int_{-\infty}^{\infty} p_{Z_2 \ldots Z_k \dot{Z}_2 \ldots \dot{Z}_k Y\dot{Y}\ddot{Y}} \times (z_2, \ldots, \dot{z}_k, y, 0, \dot{y}; t)\mathrm{d}z_2 \ldots \mathrm{d}z_k. \quad (38)$$

Using the standard technique of transformation of random variables, we seek the relationship between the joint pdf $p_{Z_2 \ldots Z_k \dot{Z}_2 \ldots \dot{Z}_k Y\dot{Y}\ddot{Y}}(\cdot)$ and $p_{Z_1 Z_2 \ldots Z_k \dot{Z}_1 \dot{Z}_2 \ldots \dot{Z}_k \ddot{Y}}(\cdot)$. In order to achieve this, we assume that at time t, Y and $\dot{Y}$ are functions of Z_1 and $\dot{Z}_1$ only, with all the other random variables remaining constant at $Z_2 = z_2, \ldots, Z_k = z_k, \dot{Z}_2 = \dot{z}_2, \ldots, \dot{Z}_k = \dot{z}_k$. In other words, we write

$$Y|_{Z_2 \ldots Z_k \dot{Z}_2 \ldots \dot{Z}_k} = G[Z_1],$$
$$\dot{Y}|_{Z_2 \ldots Z_k \dot{Z}_2 \ldots \dot{Z}_k} = G'\dot{Z}_1, \quad (39)$$

where, $G[\cdot]$ is the modified function when $Z_2 = z_2, \ldots, Z_k = z_k, \dot{Z}_2 = \dot{z}_2, \ldots, \dot{Z}_k = \dot{z}_k$ and G' denotes the derivative of $G[\cdot]$ with respect to Z_1. Assuming that for fixed values of $Y = y$ and $Z_2 = z_2, \ldots, Z_k = z_k, \dot{Z}_2 = \dot{z}_2, \ldots, \dot{Z}_k = \dot{z}_k$, there exists r solutions for $(Z_1, \dot{Z}_1)$ from Eqs. (35) and (36), we rewrite Eq. (38) in the form

$$p_{Y\dot{Y}\ddot{Y}}(y, 0, \ddot{y}; t) = \sum_{j=1}^{r} \int \underset{\Omega_j}{\cdots} \int \frac{1}{|\mathbf{J}_2|} p_{Z_1 \ldots Z_k \dot{Z}_1 \ldots \dot{Z}_k} (z_1^{(j)}, z_2, \ldots, z_k, \dot{z}_1^{(i)}, \dot{z}_2, \ldots, \dot{z}_k, \ddot{y}; t)\mathrm{d}z_2 \ldots \mathrm{d}z_k \mathrm{d}\dot{z}_2 \ldots \mathrm{d}\dot{z}_k. \quad (40)$$

Here, Ω_j is the domain of integration determined by the permissible set of values $(z_2, \ldots, z_k, \dot{z}_2, \ldots, \dot{z}_k)$ for each solution for $(Z_1, \dot{Z}_1)$. $\mathbf{J}_2$ is the Jacobian matrix, given by

$$\mathbf{J}_2 = \begin{bmatrix} \partial Y/\partial Z_1 & \partial Y/\partial \dot{Z}_1 \\ \partial \dot{Y}/\partial Z_1 & \partial \dot{Y}/\partial \dot{Z}_1 \end{bmatrix} = \begin{bmatrix} G' & 0 \\ G'' & G' \end{bmatrix}. \quad (41)$$

Now, the joint pdf $p_{Z_1 \ldots Z_k \dot{Z}_1 \ldots \dot{Z}_k \ddot{Y}}(\cdot)$ can be written as

$$p_{Z_1 \ldots Z_k \dot{Z}_1 \ldots \dot{Z}_k \ddot{Y}}(z_1, \ldots, z_k, \dot{z}_1, \ldots, \dot{z}_k, \ddot{y}; t) = p_{\ddot{Y}|\mathbf{Z}\dot{\mathbf{Z}}}(\ddot{y}; t) p_{\mathbf{Z}\dot{\mathbf{Z}}}(\mathbf{z}, \dot{\mathbf{z}}; t). \quad (42)$$

Since $\mathbf{Z}(t)$ is a vector of stationary, Gaussian random processes, it follows that $p_{\mathbf{Z}\dot{\mathbf{Z}}}(\cdot)$ is jointly Gaussian. From Eq. (37), it is seen that, $\ddot{Y}|_{\mathbf{Z}\dot{\mathbf{Z}}}$ is a linear sum of the components of $\ddot{\mathbf{Z}}$ and is thus Gaussian with mean and variance, given by

$$\mu_{\ddot{Y}|\mathbf{Z},\dot{\mathbf{Z}}} = \mathsf{E}\left[a + \sum_{j=1}^{k} b_j \ddot{Z}_j\right] = a + \sum_{j=1}^{k} b_j \mathsf{E}[\ddot{Z}_j], \quad (43)$$

$$\sigma^2_{\ddot{Y}|\mathbf{Z},\dot{\mathbf{Z}}} = \sum_{i=1}^{k}\sum_{j=1}^{k} \{b_i b_j (\mathsf{E}[\ddot{Z}_i \ddot{Z}_j] - \mathsf{E}[\ddot{Z}_i] E[\ddot{Z}_j])\}. \quad (44)$$

Here, $a = \sum_{i=1}^{k}\sum_{j=1}^{k} g''_{ij}\dot{z}_i\dot{z}_j$ and $b_j = g'_j$. Since $\mathbf{Z}$ constitutes a vector of zero-mean mutually independent stationary, Gaussian processes, it follows that $\mu_{\ddot{Y}|\mathbf{Z},\dot{\mathbf{Z}}} = a$ and $\sigma^2_{\ddot{Y}|\mathbf{Z},\dot{\mathbf{Z}}} = \sum_{j=1}^{k} b_j^2 \mathsf{E}[\ddot{Z}_j^2]$.

Thus, Eq. (42) can be rewritten in the form

$$p_{Z_1 \ldots Z_k \dot{Z}_1 \ldots \dot{Z}_k \ddot{Y}}(\mathbf{z}, \dot{\mathbf{z}}, \ddot{y}; t) = \frac{1}{\sqrt{2\pi}\sigma_{\ddot{Y}|\mathbf{Z},\dot{\mathbf{Z}}}} \times \exp\left[-\frac{(\ddot{y} - a)^2}{2\sigma^2_{\ddot{Y}|\mathbf{Z},\dot{\mathbf{Z}}}}\right] \prod_{j=1}^{k} p_{Z_j \dot{Z}_j}(z, \dot{z}; t), \quad (45)$$

where, $p_{Z_j \dot{Z}_j}(z_j, \dot{z}_j)$ denotes the joint pdf of Z_j and $\dot{Z}_j$. Since for stationary Gaussian processes, $Z \perp \dot{Z}$, we write

$$p_{Z_j \dot{Z}_j}(z, \dot{z}; t) = \frac{1}{2\pi\sigma_j\tilde{\sigma}_j} \exp\left[-\frac{z^2}{2\sigma_j^2} - \frac{\dot{z}^2}{2\tilde{\sigma}_j^2}\right], \quad (46)$$

where, σ_j and $\tilde{\sigma}_j$ are, respectively, the standard deviations of Z_j and $\dot{Z}_j$. Substituting Eq. (45) into Eq. (40), an approximation for the joint pdf, $p_{Y\dot{Y}\ddot{Y}}(z, 0, \ddot{z}; t)$, is obtained.

The next step in determining the pdf for peaks of $Y(t)$ lies in evaluating expressions in Eqs. (10) and (11). We first focus attention on evaluation of the integral of the type in

Eq. (11). Substituting the expressions for the joint pdf for $p_{Y\dot{Y}\ddot{Y}}(y, 0, \ddot{y}; t)$, we get

$$\kappa(z; t) = \sum_{j=1}^{r} \left\{ \int_{\Omega_j} \frac{p_{Z_1\dot{Z}_1}(z_1^{(j)}, \dot{z}_1^{(j)})}{|\mathbf{J}_2|} \psi_j(\mathbf{z}, \dot{\mathbf{z}}; t) \times \prod_{i=2}^{k} p_{Z_i\dot{Z}_i}(z_i, \dot{z}_i; t) \mathrm{d}z_2 \dots \mathrm{d}z_k \mathrm{d}\dot{z}_2 \dots \mathrm{d}\dot{z}_k \right\}, \quad (47)$$

where, the operator $|\cdot|$ indicates matrix determinant and

$$\psi_j(\cdot) = \int_{-\infty}^{0} \ddot{y} p_{\ddot{Y}|\mathbf{Z}\dot{\mathbf{Z}}}(\ddot{y}|\mathbf{Z} = \mathbf{z}, \dot{\mathbf{Z}} = \dot{\mathbf{z}}; t) \mathrm{d}\ddot{y} = -\frac{1}{2\pi} \left[-\sqrt{2}\sigma_{\ddot{Y}|\mathbf{Z},\dot{\mathbf{Z}}} \exp\left(-\frac{a^2}{2\sigma^2_{\ddot{Y}|\mathbf{Z},\dot{\mathbf{Z}}}} \right) - a\sqrt{\pi}\,\mathrm{erf}\left(\frac{a}{\sqrt{2}\sigma_{\ddot{Y}|\mathbf{Z},\dot{\mathbf{Z}}}} \right) + a\sqrt{\pi} \right]. \quad (48)$$

Here, $\mathrm{erf}(x) = (2\int_0^x \exp[-t^2/2]\mathrm{d}t)/\sqrt{\pi}$.

The constant ν_p in Eq. (11) can be evaluated from

$$\nu_p = \int_{-\infty}^{\infty} \int_{-\infty}^{0} \ddot{y} p_{Y\dot{Y}\ddot{Y}}(y, 0, \ddot{y}; t) \mathrm{d}\ddot{y} \mathrm{d}y = \int_{-\infty}^{\infty} \kappa(y; t) \mathrm{d}y. \quad (49)$$

The primary difficulties involved in evaluating $\kappa(y; t)$ in Eq. (47) are:

(a) determining the domain of integration Ω_j, defined by the possible set of solutions for $(Z_1^{(j)}, \dot{Z}_1^{(j)})$, and,

(b) evaluation of the multidimensional integrals, which are of the form

$$\kappa_j = \int_{\Omega_j} f(z_1^{(j)}, z_2, \dots, z_k, \dot{z}_1^{(j)}, \dot{z}_2, \dots, \dot{z}_k) \times \prod_{i=2}^{k} p_{Z_i\dot{Z}_i}(z_i, \dot{z}_i; t) \mathrm{d}z_2 \dots \mathrm{d}z_k \mathrm{d}\dot{z}_2 \dots \mathrm{d}\dot{z}_k, \quad (50)$$

where, $f(\cdot) = -|\mathbf{J}_2| p_{Z_1\dot{Z}_1}(z_1^{(j)}, \dot{z}_1^{(j)}; t) \psi_j(\mathbf{z}, \dot{\mathbf{z}}; t)$.

The dimension of the integrals in Eq. (50) is $2(k-1)$. In this study, we adopt a numerical strategy to overcome these difficulties. This is discussed in the following section.

6. Numerical algorithm

A crucial step in the above formulation lies in evaluating integrals of the type as in Eq. (50). Closed form solutions for the integrals are possible only for a limited class of problems. Here, we propose the use of Monte Carlo methods, in conjunction with importance sampling, to increase the efficiency, for evaluating these integrals. The integrals in Eq. (50) can be recast as

$$\kappa_j = \int_{-\infty}^{\infty} I[q(\mathbf{Z}) \le 0] f(\mathbf{Z}) \frac{p_{\mathbf{Z}}(\mathbf{z})}{h_{\mathbf{V}}(\mathbf{z})} h_{\mathbf{V}}(\mathbf{z}) \mathrm{d}\mathbf{z} = \frac{1}{N_s} \sum_{j=1}^{N_s} I[q(\mathbf{Z}_j) \le 0] f(\mathbf{Z}_j) \frac{p_{\mathbf{Z}}(\mathbf{z}_j)}{h_{\mathbf{V}}(\mathbf{z}_j)}, \quad (51)$$

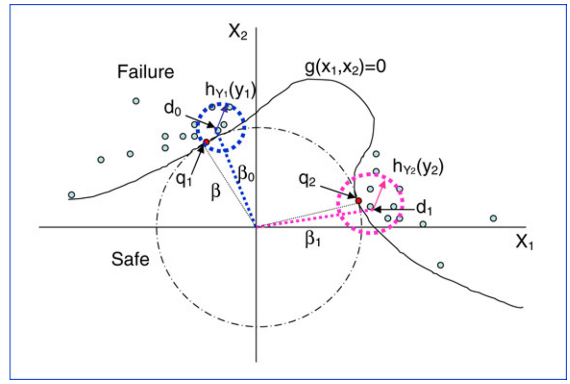

Fig. 1. Schematic diagram for numerical algorithm for evaluating multidimensional integrals; $g(x_1, x_2) = 0$ is the limit surface in the $X_1 - X_2$ random variable space; $h_{y_1}(y_1)$ and $h_{Y_2}(y_2)$ are the two importance sampling pdfs; two design points at distance β from the origin.

where, $h_{\mathbf{V}}(\mathbf{z})$ is the importance sampling pdf, N_s is the sample size used in Monte Carlo simulations and $I[\cdot]$ is an indicator function taking values of unity if $q(\mathbf{Z}) \le 0$, indicating that the sample lies within the domain of integration Ω_j, and zero otherwise. Since the problem is formulated into the standard normal space $\mathbf{Z}$, $h_{\mathbf{V}}(\mathbf{z})$ can be taken to be Gaussian with unit standard deviation and shifted mean. The difficulty, however, lies in determining where should $h_{\mathbf{V}}(\mathbf{z})$ be centered. An inspection of Eq. (51) reveals that the form of the integrals are similar to reliability integrals, which are of the form

$$\kappa_j = \int_{-\infty}^{\infty} I[q(\mathbf{Z}) \le 0] p_{\mathbf{Z}}(\mathbf{z}) \mathrm{d}\mathbf{z}. \quad (52)$$

The steps for implementing the algorithm for numerical evaluation of integrals of the type in Eq. (50) have been developed and discussed in [24,26]. The sequential steps for implementing the algorithm are detailed below, with reference to the schematic diagram in Fig. 1:

(1) Carry out pilot Monte Carlo simulations in the standard normal space. If there are too few samples in the failure domain, we carry out Monte Carlo simulations with a Gaussian importance sampling function with mean zero and a higher variance. On the other hand, if there are too few samples in the safe region, the variance of the importance sampling function is taken to be smaller. Repeat this step, till we have a reasonable number of samples in the failure and in the safe regions.

(2) We sort the samples lying in the failure domain according to their distance from the origin.

(3) A Gaussian importance sampling pdf is constructed which is centered at the sample in the failure domain lying closest to the origin. Let this point be denoted by d_0 and its distance from the origin be denoted by β_0.

(4) We check for samples in the failure domain, within a hyper-sphere of radius β_1, $\beta_1 - \beta_0 = \epsilon$, where, ϵ is a positive number.

(5) For samples lying within this hyper-sphere, we check for the sample d_1, which lie closest to the origin but are not located in the vicinity of d_0. This is checked by comparing the direction cosines of d_1 and d_0.

Fig. 2. Jack-up platform considered in numerical example.

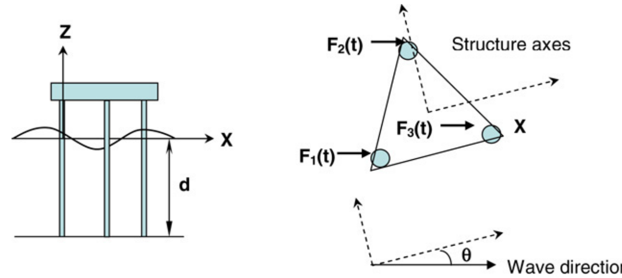

Fig. 3. Schematic diagram for the elevation and the plan views for the jack-up platform.

(6) By comparing the direction cosines of all samples lying within the hypersphere of radius β_1, we can identify the number of design points. We construct importance sampling pdfs at each of these design points. If there exists no samples with direction cosines distinctly different from d_0, there is only one design point and a single importance sampling pdf is sufficient.
(7) During importance sampling procedure corresponding to a design point, for each sample realization, we check if z_1 and $\dot{z}_1$ are real. The indicator function is assigned a value of unity if real, and zero otherwise.
(8) An estimate of κ_j is obtained from Eq. (51).

In the following section, we implement the formulation and the proposed algorithm to estimate the pdf and PDF for the response of an offshore platform subjected to sea-wave random excitations. Subsequently, we compute the mean fatigue damage rate. These predictions are compared with those obtained from the full-scale Monte Carlo simulations using an ensemble of 2000 samples.

7. Numerical example

We use the proposed formulation to estimate the fatigue damage in one of the structural members of a randomly vibrating jack-up platform. The jack-up platform considered is shown in Fig. 2. Details about the jack-up platform are available in Shabakhty [31]. The excitation loads are assumed to be only due to the sea waves acting on the structure and are taken to be random dynamic loads. In this study, we neglect the effects of wave directionality and assume that the waves act only along the axis of their propagation. The axis of the wave propagations could be assumed to act at an angle θ with respect to the reference axes of the jack-up platform; see schematic diagram in Fig. 3. Thus, under this assumption, the wave velocities acting on the three supports, and in turn, the forces developed on the supports, are all mutually correlated. The extent of correlation, however, depends on the correlation length of the water particle velocities and the physical dimensions of the structure. However, in the numerical calculations, for the sake of simplicity, we assume that the water particle velocities acting on the three supports to be mutually independent. Note that this assumption is only for ease of numerical calculations and are not restrictive since appropriate transformations, such as in Eq. (33), can always be applied to make the water particle velocities mutually independent. This simplifying assumption also enables us to make the assumption that the angle between the axis of the wave propagation and the axis of the structure to be zero. This implies that two of the supports are located symmetrically with the structure reference axis.

The water particle velocity of the sea waves are modeled as stationary Gaussian random processes and are characterized in terms of the PSD of the form

$$S_{\zeta\zeta}(\omega; z) = \frac{\omega^2 \cosh^2[2\pi(d+z)/L_w]}{\sinh^2[2\pi d/L_w]} S_w(\omega), \tag{53}$$

where, d is the water depth, L_w is the wavelength determined from the recursive relation

$$\omega^2 = \frac{2\pi g}{L_w} \tanh\left(\frac{2\pi d}{L_w}\right), \tag{54}$$

z denotes the depth under consideration, which is zero at the mean water surface level and negative below, measured vertically along the supports of the platform, and $S_w(\omega)$ is the PSD of the water surface elevations. When $z = 0$, i.e., at surface elevation, from Eq. (53), the PSD of the water particle velocity can be written as $S_{\zeta\zeta}(\omega; z = 0) = g_0^2(\omega) S_w(\omega)$, where, $g_0(\omega) = \omega \cosh[2\pi d/L_w(\omega)]/\sinh[2\pi d/L_w(\omega)]$. Here, $g_0(\omega)$ behaves as a deterministic transfer function relating the PSD of the water surface elevations to the PSD of the water particle velocities at depth $z = 0$ m. Using similar reasoning, Eq. (53) can be rewritten as

$$S_{\zeta\zeta}(\omega; z) = g_z(\omega)^2 S_w(\omega), \tag{55}$$

where, $g_z(\omega) = \omega \cosh[2\pi(d+z)/L_w(\omega)]/\sinh[2\pi d/L_w(\omega)]$ is the general form of the deterministic transfer function that relates the PSD of the water surface elevations to the PSD of the water particle velocity at depth z m. Assuming that $f(t)$ in Eq. (1) corresponds to the reference point where $z = 0$, we normalize $g_z(\omega)$ with respect to $g_0(\omega)$. Thus, one gets $\tilde{g}_z(\omega) = g_z(\omega)/g_0(\omega)$. In vector form, the water particle velocity at the different nodes of a support can be expressed as $\tilde{\mathbf{U}}(\omega) = \tilde{\mathbf{G}}(\omega) g_0(\omega) s(\omega)$, where the i-th element in $\tilde{\mathbf{U}}(\omega)$ denotes the water particle velocity corresponding to ith node at

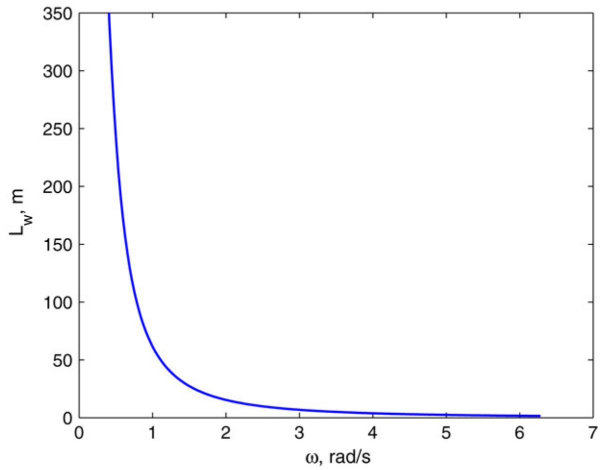

Fig. 4. Variation of L_w with ω.

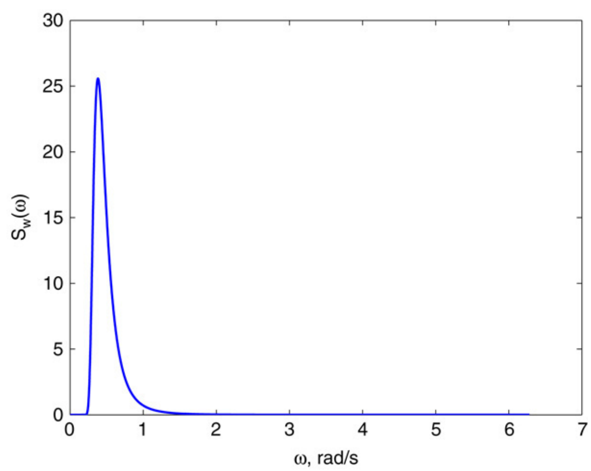

Fig. 5. The Pierson–Moskowitz spectral function for the water surface elevations.

depth z, $\tilde{g}_z(\omega)$ is the corresponding element in $\tilde{\mathbf{G}}(\omega)$ and $s(\omega)$ denotes the Fourier transform of the surface elevation which is random in time and whose PSD is given by $S_w(\omega)$. Note that $\tilde{g}_0(\omega)$ is unity for all ω.

Here, we adopt the Pierson–Moskowitz (PM) model for $S_w(\omega)$, given by

$$S_w(\omega) = \frac{4\pi^3 H_s^2}{T_z^4}\omega^{-5} \exp\left[-\frac{16\pi^3}{T_z^4}\omega^{-4}\right], \tag{56}$$

where, H_s is the significant wave height and T_z is the zero-crossing period. The numerical values considered in this example are $H_s = 10.45$ m, $T_z = 11.68$ s, d is 95 m, z is taken to vary from 0 to 95 m, $D = 2.05$ m, $\rho = 1025$ kg/m^3, $C_D = 2.777$ and $C_M = 1.824$. Fig. 4 illustrates the variation of L_w with ω, obtained by solution of Eq. (54) using the Newton–Raphson technique. The mean current speed is taken to be 0.20 m/s. Fig. 5 shows the PSD of the PM model. Here, one can see that the peak is at 0.44 rad/s and the contribution to the randomness is negligible beyond 2π rad/s. Thus, the cut-off frequency ω_c is assumed to be 2π rad/s. The PSD spectrum $S_{\zeta\zeta}(\omega)$ is discretized into 10 segments and hence $N = 10$ in Eq. (12). Since there are three identical supports, $n_s = 3$ and

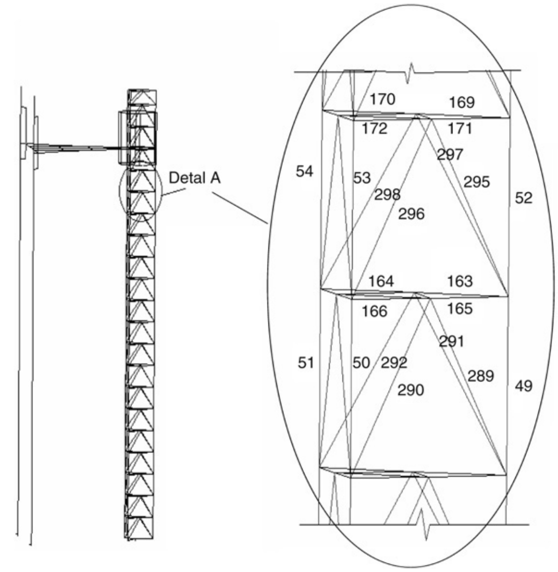

Fig. 6. Finite element model for one of the legs for the jack-up platform; a close up of the FE model is provided for the region around the element being studied (element number 295).

hence $k = 2Nn_s = 60$. Thus, the dimension of the integral in Eq. (50) is $2(k-1) = 118$.

A finite element (FE) model for the structure has been used for the vibration analysis; see Fig. 6 for the FE model for one of the legs. A commercial FE software (ANSYS) has been used for the FE analysis. More details about the FE model are available in [31]. An eigenvalue analysis of the jack-up platform reveals that the first five natural frequencies to be respectively 1.82, 1.82, 2.17, 11.26 and 12.13 rad/s. We study for the fatigue damage at a specified location of the structure. The stresses that are assumed to cause damage, designated as $\Sigma(t)$, have contributions from the axial and bending stresses, at the specified location of the structure. Since a linear structure model is assumed, $\Sigma(t)$ can be obtained as a linear function of the nodal displacements. From henceforth in the paper, $\Sigma(t)$ is analogous to $Y(t)$ in the formulation presented earlier.

We next carry out a frequency domain vibration analysis on the finite element model. A constant model damping ratio of 0.05 has been assumed for all the modes. The frequency response function (FRF) for the structure response at the desired location of the structure is computed using Eq. (20). Here, we take $\mathbf{F}_1(\omega) = \boldsymbol{\Lambda} = \tilde{\mathbf{G}}(\omega)$. It is pertinent to note here that the vector $\boldsymbol{\Lambda}$ in the time domain is not a constant but a complicated function in time. For the computation, we first carry out an eigenvalue analysis and extract the first 50 natural modes, with the 50-th natural frequency being 111.03 rad/s. Subsequently, the frequency response functions are computed from a modal analysis where the first 50 modes are considered. Since the cut-off frequency $\omega_c = 6.28$ rad/s, it can be assumed that neglecting the effect of modes beyond the 50-th one has negligible effect on the structure response. Figs. 7 and 8 show the amplitude and phase of the frequency response functions $H_i(\omega)$ at the specified location of the structure, under the action of loads acting on the i-th ($i = 1, 2, 3$) support of the jack-up platform. From Fig. 7, one can see that peaks are observed

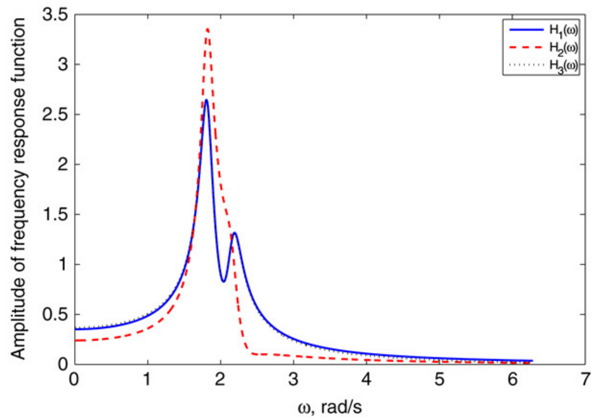

Fig. 7. Magnitude of the frequency response function at the specified location of the jack-up platform; the subscript j in $H_j(\omega)$ denotes the transfer function when the loads act only at the jth support.

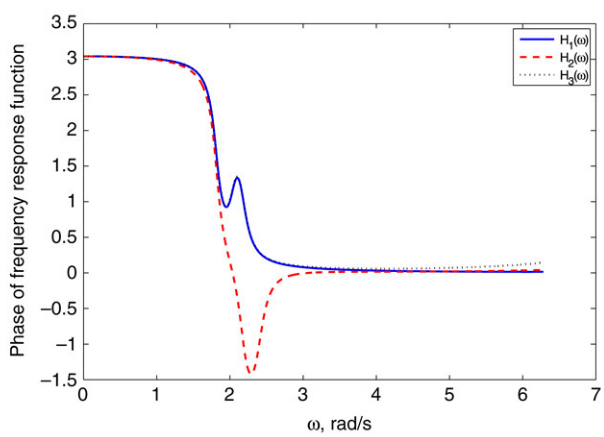

Fig. 8. Phase of the frequency response function t the specified location of the jack-up platform; the subscript j in $H_j(\omega)$ denotes the transfer function when the loads act only at the jth support.

at 1.81 and 2.17 rad/s and these correspond to the first three natural frequencies of the structure. Since the fourth natural frequency is greater than ω_c, we consider only the effect of the first three natural frequencies in analyzing the structure. It must be remarked that $H_1(\omega)$ and $H_3(\omega)$ are almost identical owing to the symmetrical nature of the structure with respect to the excitation loads. Fig. 9 shows the PSD of the linear part of the structure response when the forces on only one of the supports is considered. We observe that the response PSD has three significant peaks, which correspond to the dominant excitation frequency and the first three natural frequencies.

As discussed before, the structure response of interest, $\Sigma(t)$, is a nonlinear function of the excitations and is hence non-Gaussian. Fig. 10 shows a sample time history of the response obtained using the formulation presented in Section 3. It can be seen that though the linear part of the response has the dominant contribution to the total response, the quadratic corrections are quite significant. An ensemble of 2000 time histories of the response have been digitally generated using Monte carlo simulations, following the formulation presented in Section 3. The pdf of $\Sigma(t)$, at a particular time instant, is shown in Fig. 11. Fig. 12 shows the pdf of $\Sigma(t)$, at a particular time instant t,

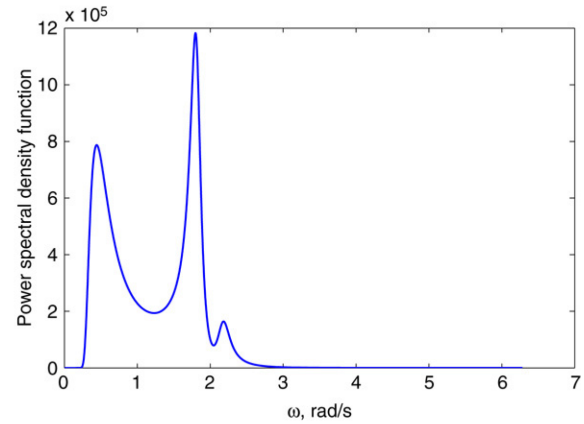

Fig. 9. Power spectral density function of the linear part of the structure response, when forces act only at one of the supports.

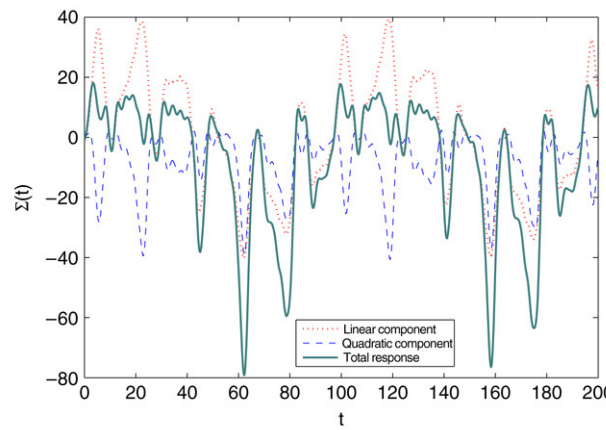

Fig. 10. Sample time history of response $\Sigma(t)$ at the specified location.

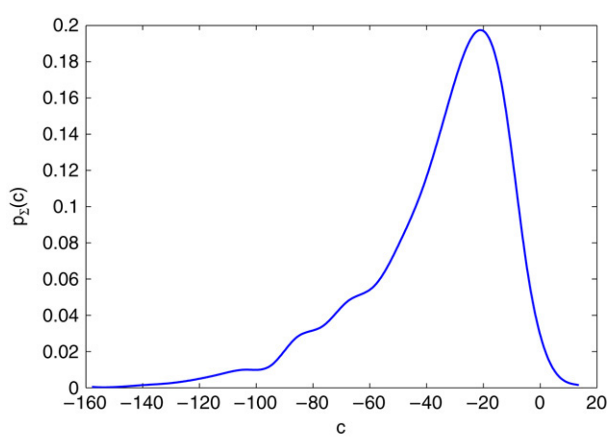

Fig. 11. Probability density function of $\Sigma(t)$ at a particular time instant; Monte Carlo simulations using 2000 samples.

drawn on the normal probability axis. Here, a sample with Gaussian distribution will be a straight line; see the dashed line. Thus, from Figs. 11 and 12, it is quite clear that the structural response shows significant non-Gaussian characteristics.

We next develop a numerical approximation for the pdf of the peaks for the response $\Sigma(t)$, using the method proposed in this paper. In implementing the proposed method numerically,

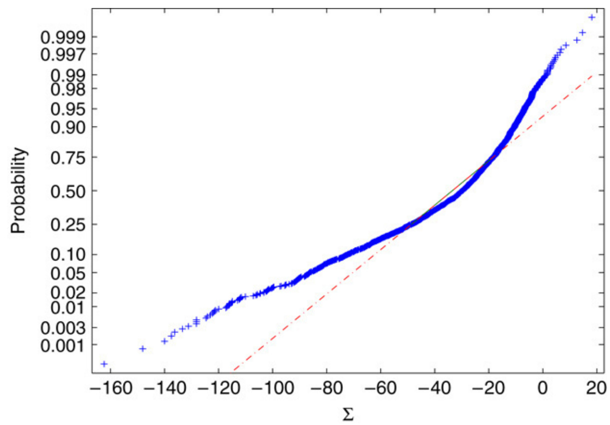

Fig. 12. Normal probability plot of $\Sigma(t)$ at a particular time instant; Monte Carlo simulations using 2000 samples.

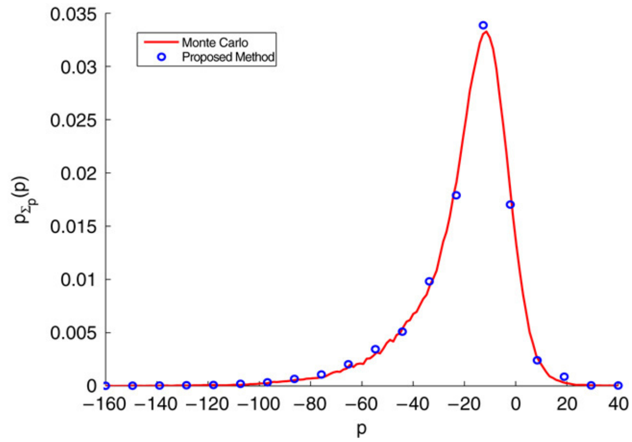

Fig. 13. Probability density function for the peaks of $\Sigma(t)$.

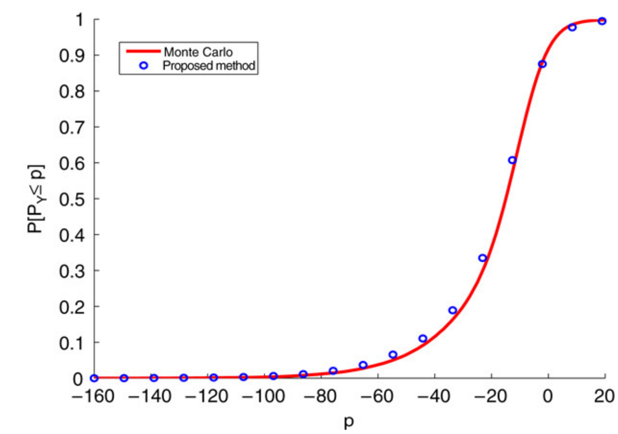

Fig. 14. Probability distribution function for the peaks of $\Sigma(t)$.

there are two primary difficulties: (a) determining the solution set $(Z_1^{(j)}, \dot{Z}_1^{(j)})$ which satisfies Eq. (39), and (b) numerically determining the domain of integration Ω_j, in Eq. (50). An inspection of Eq. (30) reveals that a solution for $Z_1^{(j)}$ can be obtained by solving a quadratic equation of the form

$$\alpha_1 Z_1^2 + \alpha_2 Z_1 + \alpha_3 = 0, \tag{57}$$

where, the constants α_i, $(i = 1, 2, 3)$ depend on whether $u(t) > 0$ or $u(t) < 0$. Thus, from Eq. (57), we see that there are two Z_1 solutions for each of the two cases when $u(t) > 0$ and when $u(t) < 0$. It is therefore quite obvious, that for a given level $\Sigma(t) = y$, there exists four solutions for Z_1, not all of which lie within Ω_j. Now, one can see that real solutions for Z_1 are obtained only when $\alpha_2^2 - 4\alpha_1\alpha_3 \geq 0$. This condition, in conjunction with the check whether a particular real solution also satisfies the condition on the sign of $u(t)$ which has been used to calculate the constants α_i, defines numerically the domain of integration Ω_j. Admissible solutions for $\dot{Z}_1$ are obtained next from Eq. (39) using the admissible solutions for Z_1 and knowing that a peak occurs when $\dot{Y} = 0$.

The next step involves computing the 118-dimensional integrals of the form as in Eq. (50). As discussed in Section 6, we use an importance sampling based Monte Carlo simulation procedure for evaluating these integrals. In implementing the numerical algorithm, we consider a sample size of 2×10^5 values. The pdf for the peaks of $\Sigma(t)$, using the proposed method, has been shown in Fig. 13. The corresponding PDF is shown in Fig. 14.

The validity of these predictions is compared with the predictions obtained from full scale Monte Carlo simulations, which are assumed to be the benchmark. In the Monte Carlo procedure, we first digitally generate an ensemble of 2000 time histories for $\Sigma(t)$, using the formulation in Section 3. Next, we use the WAFO toolbox [32], to identify the peaks corresponding to each sample time history. Subsequently, we construct the pdf for the peaks of $\Sigma(t)$, by statistically processing the peaks for the entire ensemble. These constructs for the pdf and PDF serve as the benchmark with which we compare the analytical predictions obtained from this study. As can be seen from Figs. 13 and 14, the predictions compare reasonably well with those obtained from Monte Carlo simulations.

Next, we predict the expected fatigue damage using the peak counting method. For the purpose of illustration, we consider hypothetical values of the parameters $\alpha = 10^{-4}$ and $\beta = 2.0$. Using Eq. (9) for estimating the expected fatigue damage rate, we get $\mathsf{E}[d] = 1.45 \times 10^{-4}$ when we use the estimates for the peak pdf that were obtained analytically. On the other hand, in the Monte Carlo procedure, we get $\mathsf{E}[d] = 1.15 \times 10^{-4}$. The difference is about 26% and is independent of the time duration of interest. The size of the error depends to some extent on the small errors in estimating the peak pdf. However, in this case, the primary source of error could be that of the 20 points at which the peak pdf has been estimated, only four of these points lie in the region where the peaks are positive; see Fig. 13. This introduces errors both in the calculation of $\tilde{\nu}_p$ and $\mathsf{E}[d]$.

Estimating the peak pdf at 20 points requires a fraction of the computational cost in comparison with the case when Monte Carlo simulations are used. Increasing the number of points where the peak pdf is estimated would increase the computational cost. It must also be remarked that the Monte Carlo technique is often the only solution technique involving complicated problems. Nevertheless, the proposed method offers an alternative and fast solution for estimating an approximation of the fatigue damage. The method proposed in this paper needs to be viewed in this light.

8. Concluding remarks

A methodology has been developed for approximating the probability density and distribution functions for the peaks of the stresses developed in a randomly vibrating jack-up platform, subjected to non-Gaussian time varying loads. The water surface elevation is modeled as a stationary, Gaussian random process. The resulting forces acting on the structure, calculated using the well-known Morison's equations, are non-Gaussian. The structure behaviour is assumed to be linear. Random vibration principles, in conjunction with the finite element method, are used to determine the probabilistic characteristics of the response quantities, such as stress and displacements in a particular location of the structure. These response quantities are modelled as random processes. Using theories of random processes, analytical expressions are developed for the distribution of the peaks of these random quantities. These information, in turn, is subsequently used to estimate the expected fatigue damage, according to the peak counting method. The analytical predictions are compared with those obtained from Monte Carlo simulations which serve as the benchmark. The computational effort involved in the proposed analytical method is significantly less than the Monte Carlo procedure. The savings in the CPU time however depends on the number of points at which the peak pdf is evaluated. In the numerical example where the peak pdf has been evaluated at 20 points, the savings in the computational cost is about 40%.

A key feature in the development of the proposed method lies in the assumption that for high thresholds, the number of level crossings of a non-Gaussian process can be modelled as a Poisson point process. The assumption of the outcrossings being Poisson distributed has been proved to be mathematically valid for Gaussian processes when the thresholds asymptotically approach infinity [33]. However, it has been pointed out that for threshold levels of practical interest, this assumption results in errors whose size and effect depend on the bandwidth of the processes [34]. While it can be heuristically argued that for high thresholds, the outcrossings of non-Gaussian processes can be viewed to be statistically independent and hence can indeed be modeled as a Poisson point process, to the best of the authors' knowledge, studies on the validity of this assumption, do not exist in the literature. The approximations developed in this paper, is thus expected to inherit the associated inaccuracies and limitations due to this assumption.

The number of random variables entering the proposed formulation depends on the number of terms used for discretizing the PSD for the wave velocities (see Eq. (12)). For accurate representation of the discretized PSD, the number of terms required is often quite large (about 500 or more). This can lead to potential computational problems. However, using geometric transformations proposed in the literature [35], it is possible to represent the structure response in terms of much fewer random variables. Typically, for tolerance errors of 0.1% in the representation of the variance of response, the number of random variables required could be as low as 20–40, even when the excitation PSD is discretized using 1000 random variables. This technique has, however, not been employed in the numerical example presented in this paper.

Some other simplifying assumptions considered in this study have been to neglect the effects of the relative movement of the structure with respect to the water velocities and to assume that the structure behaviour is linear. The former assumption merely simplifies the expressions and is not restrictive to the proposed method. On the other hand, considering structural nonlinear behaviour raises difficulties in treatment of the problem in the frequency domain as has been discussed in this paper. A further limitation of this study is that the Palmgren–Miner's rule parameters, α and β, have been considered to be deterministic. This however is not very restrictive and methods have been discussed in the literature which take into account the effect of randomness in structural properties; see for example [36].

It is to be emphasized here that expected fatigue damage can be calculated using various techniques proposed in the literature. It has been shown in the literature that the peak counting method overestimates the fatigue damage and serves as an upper bound for the fatigue damage. Moreover, in realistic structures, the fatigue damage usually takes place due to multi-axial stresses. This however, requires the use of alternative and more involved techniques, such as, the critical plane approaches [37–39]. Some studies involving predicting the fatigue damage due to hot-spot stresses or the Von Mises stresses have been reported in the literature [35,40–42]. Extension of some of these techniques to the present problem is not very difficult.

References

[1] Hasselman K. On the nonlinear energy transfer in a gravity-wave spectrum, part 1: General theory. Journal of Fluid Mechanics 1962;12: 481–500.
[2] Longuet-Higgins MS. The effect of nonlinearities on statistical distributions in the theory of sea wave. Journal of Fluid Mechanics 1963; 17(3):459–80.
[3] Langley RS. A statistical analysis of nonlinear random waves. Ocean Engineering 1987;14(5):389–407.
[4] Hu SLJ, Zhao D. Kinematics of nonlinear waves near free surface. Journal of Engineering Mechanics ASCE 1992;118(10):2072–86.
[5] Machado U. Probability density functions for nonlinear random waves and responses. Ocean Engineering 2003;30:1027–50.
[6] Winterstein SR. Nonlinear vibration models for extremes and fatigues. Journal of Engineering Mechanics ASCE 1988;114(10):1722–90.
[7] Ochi MK, Anh K. Probability distribution applicable to non-Gaussian random processes. Probabilistic Engineering Mechanics 1994;9:255–64.
[8] Naess A, Johnson JM. Response statistics of nonlinear, compliant offshore structures by the path integral solution method. Probabilistic Engineering Mechanics 1993;8:91–106.
[9] Naess A. Crossing rate statistics of quadratic transformation of Gaussian process. Probabilistic Engineering Mechanics 2001;16:209–17.
[10] Moarefzadeh MR, Melchers RE. Sample specific linearization in reliability analysis of offshore structures. Structural Safety 1996;18(2–3): 101–22.
[11] Moarefzadeh MR, Melchers RE. Nonlinear wave theory in reliability analysis of offshore structures. Probabilistic Engineering Mechanics 2006;21(2):99–111.
[12] Malhotra AK, Penzien J. Non-deterministic analysis of offshore structures. Journal of Engineering Mechanics Division ASCE 1970;96(6): 985–98.

[13] Donley MG, Spanos PD. Dynamic analysis of nonlinear structures by the method of statistical quadratization. Lecture notes in engineering, vol. 5. Berlin: Springer-Verlag; 1990.
[14] Naess A, Ness GM. Second-order sum-frequency response statistics of tethered platforms in random waves. Applied Ocean Research 1992;14(2): 23–32.
[15] Winterstein SR, Ude TC, Martinsen T. Volterra models in ocean structures: Extremes and fatigue reliability. Journal of Engineering Mechanics ASCE 1994;120(6):1369–85.
[16] Li XM, Quek ST, Koh CG. Stochastic response of offshore platforms by statistical cubicization. Journal of Engineering Mechanics ASCE 1995; 121(10):1056–68.
[17] Paik I, Roesset JM. Use of quadratic transfer functions to predict response of tension leg platforms. Journal of Engineering Mechanics ASCE 1996; 122(9):882–9.
[18] Grigoriu M. Applied non-Gaussian processes. Engelwood Cliffs (New Jersey): Prentice Hall; 1995.
[19] Madsen HO, Krenk S, Lind NC. Methods of structural safety. Engelwood Cliffs: Prentice-Hall; 1986.
[20] Sobczyk K, Spencer BF. Random fatigue: From data to theory. San Diego: Academic Press; 1992.
[21] Lin YK. Probabilistic theory of structural dynamics. New York: Mc-Graw Hill; 1967.
[22] Nigam NC. Introduction to random vibrations. Massachusetts: MIT Press; 1983.
[23] Lutes LD, Sarkani S. Random vibrations: Analysis of structural and mechanical systems. Butterworth-Heineman: Elsevier; 2004.
[24] Gupta S, van Gelder P. Probability distribution of peaks for nonlinear combination of vector Gaussian loads. Journal of Vibrations and Acoustics, ASME [in press].
[25] Naess A. Prediction of extremes of stochastic processes in engineering applications with particular emphasis on analytical methods. Ph.D. thesis. Trondheim: Norwegian Institute of Technology; 1985.
[26] Gupta S, van Gelder P. Extreme value distributions for nonlinear transformations of vector Gaussian processes. Probabilistic Engineering Mechanics 2007;22:136–49.
[27] Nigam NC, Narayanan S. Applications of random vibrations. Berlin: Springer-Verlag; 1994.
[28] Tovo R. Cycle distribution and fatigue damage under broad-band random loading. International Journal of Fatigue 2002;24:1137–47.
[29] Rychlik I. Note on cycle counts in irregular loads. Fatigue and Fracture in Engineering Materials and Structures 1993;16(4):377–90.
[30] Rice SO. A mathematical analysis of noise. In: Wax N, editor. Selected papers in random noise and stochastic processes. Dover Publications; 1954. p. 133–294.
[31] Shabakhty N. Durable reliability of jack-up platforms. Ph.D. Thesis. The Netherlands: Technical University of Delft; 2004.
[32] Brodtkorb PA, Johannesson P, Lingren G, Rychlik I, Ryden J, Sjo E. WAFO- A MATLAB toolbox for analysis of random waves and loads. In: Proceedings of the 10th international offshore and polar engineering conference, vol. 3. 2000. p. 343–50.
[33] Cramer H. On the intersections between the trajectories of a normal stationary stochastic process and a high level. Arkive of Mathematics 1966;6:337–49.
[34] Vanmarcke E. Properties of spectral moments with applications to random vibrations. Journal of Engineering Mechanics ASCE 1972;98:425–46.
[35] Gupta S, Rychlik I. Rainflow fatigue damage due to nonlinear combination of vector Gaussian loads. Probabilistic Engineering Mechanics. under review.
[36] Gupta S, Manohar CS. Reliability analysis of randomly vibrating structures with parameter uncertainties. Journal of Sound and Vibration 2006;297:1000–24.
[37] Socie D. Multiaxial fatigue damage models. Journal of Engineering Materials and Technology 1987;109:293–8.
[38] Socie D. Critical plane approaches for multiaxial fatigue damage assessment. In: McDowell DL, Ellis R, editors. Advances in multiaxial fatigue. American Society for Testing and Materials; 1993. p. 7–36.
[39] You BR, Lee SB. A critical review on multiaxial fatigue assessment of metals. International Journal of Fatigue 1996;18(4):235–44.
[40] Rychlik I, Gupta S. Rainflow fatigue damage for transformed Gaussian loads. International Journal of Fatigue 2007;29:406–20.
[41] Preumont A, Piefort V. Predicting random high-cycle fatigue life with finite elements. Journal of Vibration Acoustics 1994;116:2458.
[42] Pitoiset X, Preumont A. Spectral methods for multiaxial random fatigue analysis of metallic structures. International Journal of Fatigue 2000;22: 54150.